Developments in Relativistic Nonlinear Optics

D. Umstadter, S. Banerjee, S. Chen, E. Dodd, K. Flippo, A. Maksimchuk, N. Saleh, A. Valenzuela, and P. Zhang

Center for Ultrafast Optical Science, 1006 IST Bldg., University of Michigan, Ann Arbor 48109-2099

Abstract. We report recent results of experiments and simulations in the regime of peak laser intensities above 10^{19} W/cm^2, including the following topics: (1) electron and proton acceleration to energies in excess of 10 MeV in well collimated beams; (2) use of laser chirp to control the growth of plasma waves and acceleration of electrons by the Raman instability; (3) all optical injection and acceleration of electrons; (4) relativistic self-focusing by means of the mutual index of refraction of two overlapping laser pulses; (5) creation of a radioisotope by the reaction $^{10}\mathrm{B}(d,n)^{11}\mathrm{C}$; (6) high-order harmonic generation from relativistic free electrons in an underdense plasma.

INTRODUCTION

In the last decade, table-top lasers have undergone an orders-of-magnitude jump in peak power, with the invention of the technique of chirped pulse amplification [1]. They now have multi-terawatt peak powers and, when focused, can produce electromagnetic intensities well in excess of 10^{18} W/cm^2, which is high enough to cause nonlinearity with even unbound (ionized) electrons [2]. The nonlinearity arises, in this case, because the electrons oscillate at relativistic velocities in laser fields that exceed 10^9 V/cm, resulting in relativistic mass changes exceeding the electron rest mass and the light's magnetic field becomes important. The work done on an electron over the distance of a laser wavelength (λ) then approaches the electron rest mass energy ($m_e c^2$),where m_e is the electron rest mass and c is the speed of light. Thus, a new field of nonlinear optics, that of relativistic electrons, has been launched. Effects analogous to those studied with conventional nonlinear optics—self-focusing, self-modulation, harmonic generation, and so on—are all found, but based on this entirely different physical mechanism. Applications of these phenomena include compact and ultrashort pulse duration laser-based electron accelerators and x-ray sources.

In this paper, the results of our recent simulations and experiments are discussed in the following order: first, acceleration of electrons that are self-trapped; next, a technique to control the Raman instability by use of chirped pulses; then, some preliminary experiments in which one laser pulse injects electrons from the plasma into the plasma wave created by another. In the next section: proton acceleration, including the production of a short-lived radioisotope. Following that: high-order harmonic generation. Lastly: prospects for applications.

CP611, *Superstrong Fields in Plasmas:* Second Int'l. Conf., edited by M. Lontano et al.

ELECTRON ACCELERATION

For time periods that are short compared to an ion period, electrons are displaced from regions of high laser intensity, but ions, due to their much greater inertia, remain stationary. The resulting charge displacement provides an electrostatic restoring force that causes the plasma electrons to oscillate at the plasma frequency (ω_p) after the laser pulse passes by them, creating alternating regions of net positive and negative charge. The resulting electrostatic wakefield plasma wave propagates at a phase velocity nearly equal to the speed of light and thus can continuously accelerate properly phased electrons.

Acceleration of electrons by electron plasma waves is of current interest because the acceleration gradient (200 GeV/m) is much larger (four orders of magnitude larger) than in conventional rf linacs ($<$ 20 MeV/m) [3, 4]. Several methods have been proposed for driving a large-amplitude high-phase-velocity plasma wave, such as the plasma wake-field accelerator, the plasma beat-wave accelerator, the laser wake-field accelerator (LWFA) and the self-modulated laser wake-field accelerator (SMLWFA). The LWFA and the SMLWFA have received considerable attention and shown rapid progress because of the development of table-top ultrashort-duration terawatt-peak-power lasers. In the SMLWFA, an electromagnetic wave (ω_o, k_o) decays into a plasma wave (ω_p, k_p) and another forward-propagating light wave ($\omega_o - \omega_p, k_o - k_p$) via the stimulated Raman forward scattering instability. In this case, the laser pulse duration is longer than an electron plasma period, $\tau >> \tau_p = 2\pi/\omega_p$.

We have recently studied theoretically the coherent control of the Raman-driven plasma waves by the use of a frequency chirp on the laser beam. Theoretical calculations show that a 12% bandwidth will eliminate Raman forward scattering for a plasma density that is 1% of the critical density. We find analytically that the amount of chirp needed to eliminate SRS,

$$b = -\frac{1}{4}\frac{\omega_0}{\omega_e}\frac{\gamma_0}{\tau_p}, \tag{1}$$

where ω_0 is the incident light's frequency, ω_e is the plasma wave frequency, τ_p is the full-width-half-maximum length of a pulse with a Gaussian profile, and γ_0 is the growth rate. The bandwidth for a chirped pulse can be written as $\Delta\omega_0 \simeq 2b\tau_p \simeq 1/2(\omega_0/\omega_e)\gamma_0$. The predicted changes to the growth rate are confirmed in two-dimensional particle-in-cell simulations. As shown in Fig. 1, a positive chirp (c) is found to increase the growth of Raman-driven plasma waves as compared with no chirp (a); a negative chirp (b) is found to decrease it [6]. In the LWFA, an electron plasma wave is driven resonantly by a short laser pulse ($\tau \sim \tau_p$) through the laser ponderomotive force. Self-guiding is possible when laser power exceeds the threshold for relativistic self-guiding, P_c. Whole beam self-focusing and, more recently, relativistic filamentation (a partial beam analog to the whole beam effect, or multiple filaments) have both been observed [5].

Several labs have observed the acceleration of MeV electrons by the SMLWFA, sometimes accompanied by self-guiding, but with large-electron energy spreads (most of the electrons have energies less than 5 MeV, with the number decaying exponentially with a temperature of $\sim$ 1 MeV to just a few electrons at energies up to 100 MeV). The origin of the accelerated electrons is a subject of some debate. It has been attributed to

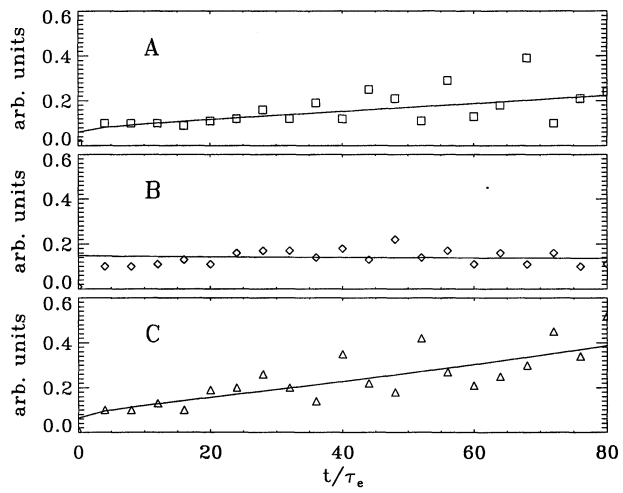

FIGURE 1. The amplitude of the density perturbations are plotted as a function of time. Plot A is the unchirped pulse, B, negatively, and C, the positively chirped pulses.

catastrophic wave-breaking of a relativistic Raman forward scattered plasma wave, and to wavebreaking of slower velocity Raman backscattered waves in both experiment and theory. A two-temperature distribution in the electron energy spectrum was observed [7] to accompany a multi-component spatial profile of the electron beam. In this case, electrons in the low energy range were observed to undergo an abrupt change in temperature, coinciding with the onset of extension of the laser channel due to self-guiding of the laser pulse, when the laser power or plasma density was varied. With the aid of a test-particle simulation, we have now determined that both of these effects appear to originate from the dynamics of trapping and detrapping as electrons oscillate in their orbits in the seperatrix from regions of acceleration to decelleration and from defocusing to focusing [7].

Laser acceleration of electrons is illustrated in Fig. 2. Here, an intense laser interacts with a gas jet located inside a vacuum chamber. The laser crosses the picture from left to right and is focussed by a parabolic mirror (right side of the picture). The supersonic nozzle (shown in the middle of the picture) is positioned with micron accuracy with a 3-axis micropositioner. The e-beam (up to 10^{10} electrons per shot) makes a small spot on a fluorescent (LANEX) screen (imaged with a CCD camera), shown in the upper left-hand corner of the picture. As shown in Fig. 2 [7], as the laser power increases, the divergence angle of the electron beam decreases. The lowest angle, 1°, obtained at the highest power, corresponds to a transverse geometrical emittance of $\varepsilon_{\perp} \leq 0.06\pi$ mm-mrad [7], which is an order of magnitude lower than that from the best conventional electron gun. This may be because a large acceleration gradient decreases the time over which space-charge can act to degrade the emittance.

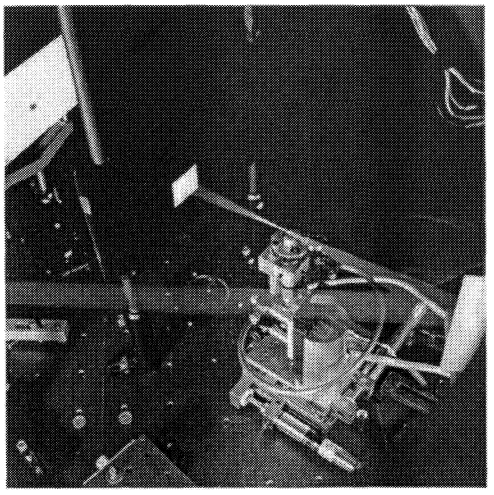

FIGURE 2. Photograph of the acceleration of an electron beam by a laser interacting with a gas jet inside a vacuum chamber. The laser (illustrated for the purpose of orientation) crosses the picture from left to right and is focused by a parabolic mirror (right side of the picture). The supersonic nozzle (shown in the middle of the picture) is position with micron accuracy with a 3-axis micropositioner. The e-beam makes a small spot on a white florescent (LANEX) screen, shown in the upper left-hand corner of the picture.

Optical Injection

The injection of electrons into plasma waves can occur uncontrollably by trapping of hot background electrons, which are preheated by other processes such as Raman backscattering and sidescattering instabilities [8], or by wave-breaking (longitudinal [9] or transverse [10]). Because the electrons in this case are injected into the plasma wave uniformly in phase space, large energy spreads result, as is typically observed in the SMLWFA regime. The injection can also be controlled by use of an external electron source (such as from an RF gun); however, because the pulse durations of the injected electron bunches in the experiments in which this method was tried were longer than the acceleration buckets, the energy spread was again large. It has been shown analytically and numerically that controlled injection might also be accomplished by means internal electrons, from the plasma itself, which are all put into the accelerating phase of the plasma wave by a separate laser pulse [11, 2]. Such a laser-driven plasma-cathode electron gun might eventually have (1) monoenergetic energy, (2) GeV/cm acceleration fields, (3) micron source size, (4) femtosecond pulse duration, (5) high brightness, (6) absolute synchronization between electrons and laser (for pump and probe experiments) and (7) compact size (university-lab scale).

As a first step towards the realization of monoenergetic beams by means of optical injection, we have studied experimentally, in the SMLWFA regime, a concept first discussed in the LWFA regime [11]. By crossing in a plasma two beams, each of duration 400 fs and wavelength 1 μm, one with high vacuum intensity ($a_0 = 1.0$) and

the other lower intensity ($a_0 = 0.25$), we find that only when the beams are overlapped in space and time do we observe what appears to be diffraction of light from a standing wave (see Fig. 3) and the acceleration of electrons in the direction of the low power beam (see Fig. 4). Injection in this case is caused by the ponderomotive force of a standing

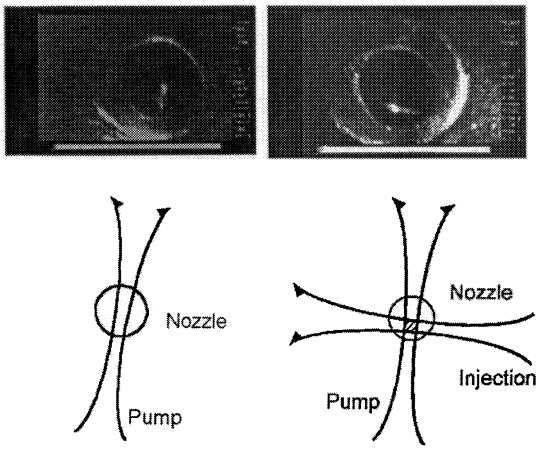

FIGURE 3. Photograph of the light Thomson scattered from the beam channels, without (left) and with (right) a crossed beam. Notice the creation of a standing wave at the bisector in the latter case.

wave created along the bisector of the two beams, which will stochastically heat the electrons to relativistic temperature and allow them to be caught in the plasma wave that was created by the low power beam. This process is similar to the "preheating" that occurs when the slow-phase-velocity plasma wave driven by Raman backscattering injects electrons into the faster plasma waves that are generated by Raman forward scattering [8]. However, in this case, the ponderomotive force of the standing wave is much higher because of its much shorter wavelength. It is also occasionally observed that the increase of the index of refraction resulting from the addition of the pulses can extend the distance over which the low-power beam remains focused. This is the first time that one laser beam has been used to trigger the acceleration of electrons by another laser beam, thus proving the LILAC principle.

PROTON ACCELERATION

Plasma ions can be accelerated to high energies by the formation of an electrostatic sheath due to charge displacement. The latter results from the initial preferential acceleration of electrons; the heavier ions are left behind due to inertia. Ions will also be accelerated by each other's unshielded charges in what has been termed a "Coulomb explosion." Among the many mechanisms that can accelerate the electrons are: thermal expansion, plasma waves, "$J \times B$ heating" or "vacuum heating." Recent simulations reveal a new mechanism [12] that occurs in cases where a significant preplasma exists, such as for pulses with typical laser-intensity contrast ratios. In this case, a standing wave is produced by the beating of the incident and reflected light, which can heat the

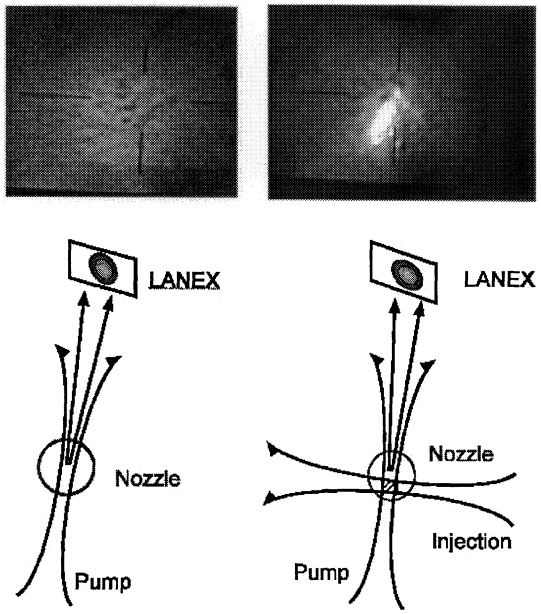

FIGURE 4. Photographs of the spatial profile of a laser accelerated electron beams without (left) and with (right) injection.

electrons to relativistic temperatures, as was described in the discussion of optical injection.

Energetic ions from underdense plasmas were accelerated by an electrostatic sheath, which was created by charge-displacement. Unlike earlier long-laser-pulse experiments, the displacement was due not to thermal expansion but to ponderomotive blow-out [13, 14]. When a helium-gas was used as the target, alpha particles were accelerated to several MeV in the direction orthogonal to the direction of laser propagation and along the direction of the maximum intensity gradient.

Several groups have reported the observation of ions originating from thin-film solid-density targets (or protons originating from monolayers of water on the target surface). Unlike previous long-pulse experiments, the protons were accelerated along the direction normal to the side of the target opposite to that upon which the laser was incident. The laser is focused with an off-axis parabola onto a thin-foil, held by a mesh that is positioned by a 3-axis micropositioner. A nuclear track detector, CR-39 , is used to measure the proton-produced pattern [15]. For instance, Fig. 5 shows the difference in the spatial profile of between a mylar target, an insulator, and aluminum, a conductor. Note that the proton beam from the latter is much smoother. In another experiment, protons were observed to be emitted in ring patterns, the radii of which depend on the proton energy, which was explained by self-generated magnetic fields [16]. Another recent result reported proton energies up to 60 MeV [17]. The results of these experiments indicate that a large number of protons (10^{13} p) can be accelerated, corresponding to current densi-

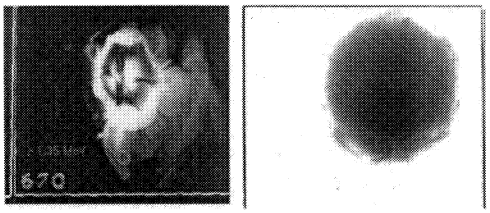

FIGURE 5. Photograph of the spatial profile of a laser accelerated proton beams from a mylar target (left) and aluminum target (right). The proton beam is detected with CR-39, a nuclear track detector.

ties (10^8 A/cm^2) at the source that are nine orders-of-magnitude higher than produced by cyclotrons, but with comparable transverse emittances ($\varepsilon_\perp \leq 1.0\pi$ mm-mrad). The high end of the energy spectrum typically has a sharp cut-off, but, like the electrons is a continuum.

While the protons in several experiments originate from the front-side of the target [15, 16], in another [17], they originate from the back-side. Evidence for a back-side origin comes from results obtained when wedge-shaped targets were used. The proton beam was observed to point in the direction normal to the back side of the target, which was not perpendicular to the front surface. On the other hand, evidence for a front-side origin comes from an experiment in which deuterium was coated on a thin film of mylar and a boron target was placed behind it [18].

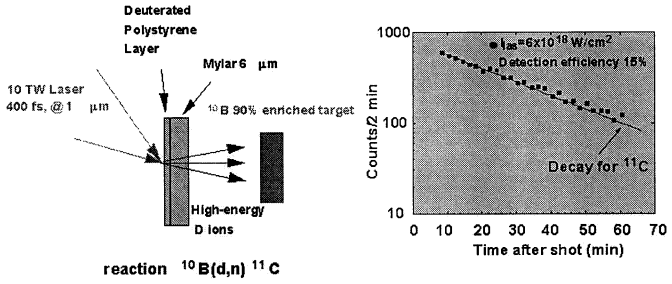

FIGURE 6. Experimentally recorded radioactive decay rate corresponds to that of ^{11}C, which decays by positron emission. The 511 keV gamma rays which were detected were created by annihilation of the electron-positron pairs.

High-order Harmonic Generation from Free Electrons

We report the first observation of high harmonics generated due to the scattering of relativistic electrons from high intensity laser light. The experiments were carried out with an Nd:Glass laser system with a peak intensity of 10^{19} W/cm^2 in underdense plasma. At high intensities, when the normalized electric field approaches unity, in addition to the conventional atomic harmonics from bound electrons, there is significant contribution to the harmonic spectrum from free electrons. The characteristic signatures of this are

found to be the emission of even order harmonics (see Fig. 7), linear dependence on the electron density, significant amount of harmonics even with circular polarization and a much smaller spatial region over which these harmonics are produced (and emitted in a narrower cone) as compared to the atomic case. Imaging of the harmonic beam shows that it is emitted in a narrow cone with a divergence of 2-3 degrees.

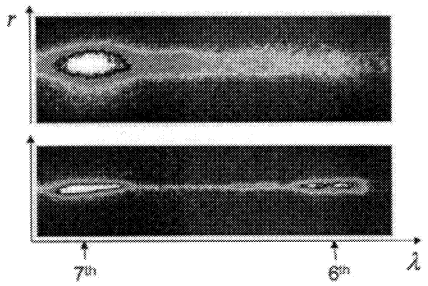

FIGURE 7. Spatial profile of the high order harmonics (a) $I = 5 \times 10^{16}$W/cm^2, $n = 10^{17}$ cm^{-3} and linear polarization (b) $I = 5 \times 10^{17}$W/cm^2, $n = 10^{18}$ cm^{-3} and circular polarization. Note that even orders appear only at high laser intensity and electron density.

PROSPECTS

Besides the beam of harmonics, discussed in the previous section, a promising avenue for the production of x-rays is based on the use of Compton scattering. Upon scattering with an electron beam, laser light can be upshifted due to a relativistic boost by a factor of $4\gamma^2$, which for electrons accelerated to 30 MeV corresponds to a factor of 10,000. Thus a 1 eV photon can be upshifted to 10 keV. Such coherent, ultrashort duration and energetic sources could enable ultrafast imaging on the atomic scale. If the source of the electron beam were a laser accelerator, the footprint of this synchrotron-like device would be small enough for it to fit in a university laboratory.

It was demonstrated that there are a sufficient number of electrons accelerated by laser-plasma accelerators to conduct pulsed radiolysis [19]. Time-resolved radiobiological studies with laser accelerated protons are also feasible.

It has been shown theoretically that a laser-induced burst of hot electrons or ions could be used as a spark to ignite a thermonuclear reaction with inertial confinement fusion in the so-called fast-ignitor laser fusion concept. In its original conception, a short but energetic laser pulse would drill through the under-dense plasma that surrounds the fusion core and a second shorter pulse would deposit energy in the core in the form of MeV electrons. In so doing, it would relax the otherwise stringent requirements on energy and symmetry of the long-pulse-duration heating and compression pulses. More recently, the use of a short pulse of ions for the ignitor has also been discussed.

The short-lived radioactive isotopes that were produced by laser acceleration of ions might be used to for cancer diagnostics such as in positron-emission tomography. Because they are created impulsively with a ion short pulse, they might also be used to study ultrashort duration isotope decay times in nuclear physics. If protons could be

laser-accelerated to 70-160 MeV energies, they could be useful for proton therapy, which is now limited by the extraordinary expense of cyclotrons or synchrotrons and the large magnets required to transport the proton beams to the patient. Protons are superior to other forms of ionizing radiation for cancer treatment because of less straggling and their ability to deposit their energy over a narrower depth range.

ACKNOWLEDGMENTS

The authors acknowledge the support of the High Energy Physics Division, U.S. DOE, award DE-FG02-98ER41071 (electrons); Chemical Sciences, Geosciences and Biosciences Division, U.S. DOE (ions and x-rays); NSF (laser and plasma physics).

REFERENCES

1. Mourou, G A., Barty C P. J., and Perry, M. D., Physics Today, (Jan., 1998), and references therein.
2. Umstadter, D., Phys. Plasmas **8**, 1774 (2001), and references therein.
3. Tajima, T. and Dawson, J. M., Phys. Rev. Lett. **43**, 267, (1979).
4. Esarey, E., Sprangle, P., Krall, J., and Ting, A., IEEE Trans. Plasma Sci. **PS-24**, 252 (1996), and references therein.
5. Wang, X., Krishnan, M., Saleh, N., Wang H., and Umstadter, D., Phys. Rev. Lett. **84**, 5324 (2000).
6. Dodd, E., and Umstadter, D., Phys. Plasmas **8**, 3531 (2001).
7. Chen, S.-Y., Krishnan, M., Maksimchuk, A., Wagner, R. and Umstadter, D., Phys. of Plasmas **6**, 4739 (1999).
8. Bertrand, P., Ghizzo, A., Karttunen, S. J., Pattikangas, T. J. H., Salomaa, R. R. E., and Shoucri, M., Phys. Rev. E **49**, 5656 (1994).
9. Modena, A., Najmudin, Z., Dangor, A. E., Clayton, C. E., Marsh, K. A., Joshi, C., Malka, V., Darrow, C. B., Danson, C., Neely, D., and Walsh, F. N., Nature **377**, 606 (1995).
10. Bulanov, S. V., Pegoraro, F., Pukhov, A. M., and Sakharov, A. S., Phys. Rev. Lett. **78**, 4205 (1997).
11. Umstadter, D., Kim, J. K., and Dodd, E., Phys. Rev. Lett. **76**, 2073 (1996).
12. Sentoku, Y. et al., Appl. Phys. Letts. (submitted, 2001).
13. Sarkisov, G. S., Bychenkov, V. Yu., Novikov, V. N., Tikhonchuk, V. T., Maksimchuk, A., Chen, S. Y., Wagner, R., Mourou, G., and Umstadter, D., Phys. Rev. E **59** 7042 (1999).
14. Krushelnick, K., Clark, E. L., Najmudin, Z., *et al.*, Phys. Rev. Lett. **83**, 737 (1999).
15. Maksimchuk, A., Gu, S., Flippo, K., Umstadter, D., Bychenkov, V.Y., Phys. Rev. Lett. **84,** 4108 (2000).
16. Clark, E. L., Krushelnick, K., Davies, J. R., *et al.*, Phys. Rev. Lett. **84**, 670 (2000).
17. Snavely, R. A., Key, M. H., Hatchett, S. P., *et al.*, Phys. Rev. Lett. **85**, 2945 (2000).
18. Nemoto, K., Maksimchuk, A., Banerjee, S., Flippo, K., Mourou, G., Umstadter, D., Bychenkov, V. Yu., Appl. Phys. Lett. **78**, 595 (2001).
19. Saleh, N., Flippo, K., Nemoto, K., Umstadter, D., Crowell, R. A., Jonah, C. D., Trifunac, A. D., Rev. Sci. Instr., **71**, 2305 (2000).